

# Westerlund 1: bound or unbound?

Mengel, S • Tacconi-Garman, L.E.

© Springer-Verlag ●●●●

## Abstract

The Galactic open cluster Westerlund 1 (Wd 1) represents the ideal local template for extragalactic young massive star clusters, because it is currently the only nearby young cluster which reaches a mass of around  $\sim 10^5 M_{\odot}$ . The proximity makes spatially resolved studies of its stellar population feasible, and additionally permits direct comparison of its properties with measurements of velocity dispersion and dynamical mass for spatially unresolved extragalactic clusters.

Recently, we published the dynamical mass estimate based on spectra of four red supergiants. We have now identified six additional stars which allow a determination of radial velocity from the wavelength covered in our VLT/ISAAC near-infrared spectra (CO bandhead region near  $2.29 \mu\text{m}$ ), improving statistics significantly. Using a combination of stepping and scanning the slit across the cluster centre, we covered an area which included the following suitable spectral types: four red supergiants, five yellow hypergiants, and one B-type emission line star.

Our measured velocity dispersion is  $9.2 \text{ km/s}$ . Together with the cluster size of  $0.86 \text{ pc}$ , derived from archival near-infrared SOFI-NTT images, this yields a dynamical mass of  $1.5 \times 10^5 M_{\odot}$ . Comparing this to the mass derived via photometry, there is no indication that the cluster is currently undergoing dissolution.

**Keywords** open clusters and associations: individual: Westerlund 1 – Galaxies: star clusters – supergiants

## 1 Introduction

The concept that globular clusters may still be forming today dates back fifteen years (Holtzman et al. 1992), and ever since young massive star clusters (YMSCs) have been the focus of intense studies. First, it needed to be verified that they actually have the properties which will make them comparable to (part of) the globular clusters seen today after a Hubble time of evolution.

Once it was clear that, at least regarding mass, size and concentration, they could indeed be globular clusters in the making (Whitmore & Schweizer 1995), survival times became an issue. A fraction between 10% and around 90% of the clusters seems to dissolve in each decade of time (Fall et al. 2004; Mengel et al. 2005; Bastian et al. 2005; Whitmore et al. 2007). At least the high end of these destruction rates is in conflict with the assumption that clusters at an age of around 10 Myr, which have typically survived tens of crossing times, are in virial equilibrium.

However, only clusters which can be spatially resolved into single stars can be used to verify their dynamical state directly. The well known and comparatively numerous Galactic clusters with maximum masses of around  $10^4 M_{\odot}$  are not suitable as templates, because at an age of around 10 Myr, they are not necessarily expected to be in virial equilibrium, owing to longer crossing times, and the increased impact of interaction with galactic environment. Therefore, Wd 1 turned out to be the best-suited template in the Milky Way when it was discovered that its mass is much higher than initially (Westerlund 1961) thought, around  $\times 10^5 M_{\odot}$  (Clark et al. 2005). Given its young age of around 5 Myr, there is a considerable probability to find it in the process of disruption.

In an attempt to determine the dynamical state of Wd1, we conducted high resolution spectroscopy in the

arXiv:0803.4471v1 [astro-ph] 31 Mar 2008

---

Mengel, S  
Tacconi-Garman, L.E.  
ESO, Karl-Schwarzschild-Str. 2, 85748 Garching, Germany

near-infrared. That is the only wavelength range (because of the high extinction suffered by the cluster) which simultaneously allows a high signal-to-noise ratio, high spectral resolution, and large spatial coverage.

## 2 Observations and data reduction

Observations were conducted on VLT-ANTU on the nights of March 11 and 12, 2006 and consisted of two parts: 1) scanning the slit across a region while integrating, covering the whole field shown in Figure 1, and 2) stepping in steps of  $0''.3$ , the slit width, across the smaller region indicated by the black box in Figure 1. In both cases, the  $2'$  long slit was oriented in N-S-direction. The large spatial coverage of the scan was achieved by performing scans of three different slit positions, offset in N-S-direction by  $108''$  each time, which allows for some spatial overlap.

The central wavelength was set to be  $2.31\ \mu\text{m}$ , and the actual wavelength range covered is  $2.249 - 2.373\ \mu\text{m}$  at a resolution of  $R \approx 9000$  (the maximum resolution ISAAC allows).

Reduction of the data was performed using the IRAF package<sup>1</sup>. It included sky subtraction (a scan across an empty sky field  $10'$  away was performed with identical integration time of 300 s directly after the cluster scan, and sky positions were interleaved in the stepping observation every 10 minutes), bad pixel correction, and flatfielding.

Wavelength calibration combined the information of the XeAr lamp spectra and the night sky lines (Rousselot et al. 2000). Spatial distortion was easily corrected due to the many star spectra along the slit.

We extracted the individual spectra by averaging all the individual frames which included a star of interest, and then extracting from the combined frame by defining the aperture by hand.

For the correction of the telluric absorption features, we used the hot, featureless stars covered by the stepped spectra (for example, W42a and a star without a known designation). This gave a much better result than using the dedicated solar type telluric standards taken after the scans, which left some residuals around the MgI line.

Finally, we normalized all spectra which were used for the analysis by dividing by the continuum level determined from a small window (roughly 50 pixels) just

shortward of the CO bandhead. For the age determination, we used a rough flux calibration as an additional constraint on the spectral types. Nothing has changed for those results since Mengel & Tacconi-Garman (2007), we refer to that publication for the details.

The resulting spectra are shown in Fig. 2.

## 3 Analysis and Results

The four brightest stars are assigned spectral types ranging between M3I and M6I (foreground objects are ruled out also because of the small spread in radial velocity).

We determined the rms radial velocity dispersion of all stars where this was possible from the wavelength range covered in our observations, which limited the selection to four red supergiants, five (assumed) yellow hypergiants (YHGs), and one sgB[e] type emission line star. See Table 1 for the individual radial velocities, and also some other properties like designation, spectral type, etc.

A challenge, compared to the determination of velocity dispersion from just the RSGs, was the fact that the YHGs and the RSGs have almost no absorption lines in common at this wavelength range, and we also (currently) have no access to theoretical high-resolution spectra in the K-band for the YHGs. Therefore, we used a multi-step-procedure in an attempt to use a common wavelength reference frame for all our stars (except W9, which is a special case): First, we cross-correlated the spectrum of W237 in the region of CO absorption with the rest wavelength Arcturus spectrum from Hinkle et al. (1995). Cross-correlation of W237 with the other RSGs around the CO absorption region gave us their radial velocities relative to W237. Using W20 and W26 as reference stars, we used the Ca absorption lines between  $2.26$  and  $2.263\ \mu\text{m}$ , and the Mg line around  $2.282\ \mu\text{m}$  to determine the relative velocities of those stars with respect to W32. And finally, we used five different lines/regions (all listed in table 1) for the determination of relative velocities between W32 and the other YHGs. The radial velocity of W9 was determined by manual best fit of the S emission lines.

The resulting velocity dispersion is  $9.2 \pm 2.5\ \text{km/s}$ . Uncertainties of this value were determined through Monte Carlo simulations, using the uncertainties in the individual velocity determinations, but we added  $0.5\ \text{km/s}$  uncertainty because of the additional uncertainty in matching RSG and YHG velocity reference points.

This value is somewhat higher (even though consistent within the uncertainties) than the value we had obtained previously from the RSGs alone (Mengel & Tacconi-Garman

<sup>1</sup>IRAF is distributed by the National Optical Astronomy Observatories, which are operated by the Association of Universities for Research in Astronomy, Inc., under cooperative agreement with the National Science Foundation.

Star	Reference star	Spectral lines used	$v_{corr}$	Spectral Type
W26	W237	CO	-48.7	M5-6I
W20	W237	CO	-49.2	M5I
W75	W237	CO	-59.2	M4I
W237	Arcturus	CO	-61.7	M3I
W4	W32	lines below $2.26\mu\text{m}$ , S 2.27, Mg 2.28, C2.29	-57.8	F2Ia <sup>+</sup>
W8a	W32	lines below $2.26\mu\text{m}$ , S 2.27, Mg 2.28, C2.29	-41.9	F5Ia <sup>+</sup>
W9	W32	S emission	-62.4	sgB[e]
W12a	W32	lines below $2.26\mu\text{m}$ , S 2.27	-61.3	A5Ia <sup>+</sup>
W265	W32	lines below $2.26\mu\text{m}$ , S 2.27, C2.29	-35.5	F5Ia <sup>+</sup>
W32	W20, W26	Ca 2.26, Mg 2.28	-57.4	F5Ia <sup>+</sup>

**Table 1** Selected properties of the stars used for the measurement of the velocity dispersion: Designation as in Westerlund (1987), the star which was used as a crosscorrelation reference, the spectral lines used for the cross correlation, the heliocentrically corrected radial velocity (we applied a correction of +27.6km/s), and the spectral types (for the RSGs from Mengel & Tacconi-Garman (2007), for the other stars from Clark et al. (2005)). See text for an explanation of reference stars and spectral lines.

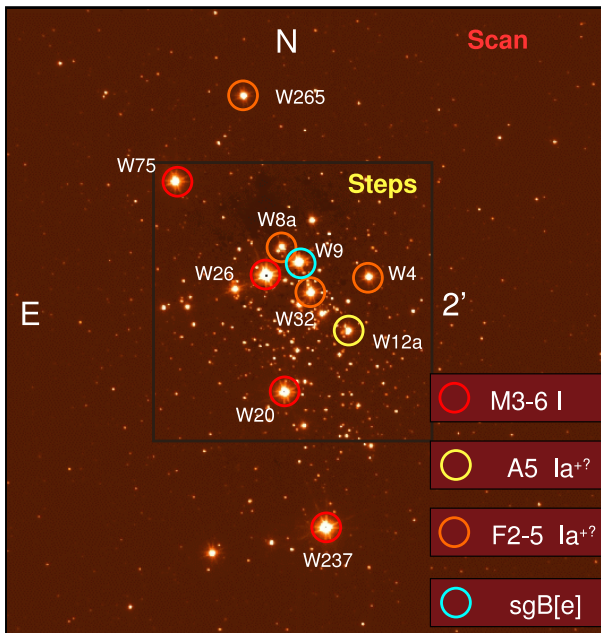


**Fig. 1** NTT/SOFI near-infrared image of Wd 1, composed from narrow band images ( $2.09\mu\text{m}$  and  $2.17\mu\text{m}$ ). The area shown was covered by the slit scans (with the slit oriented N-S), and the area shown by the black box was covered by steps of  $0''.3$  separation. Different stellar types are indicated by different coloured circles, and the stars are identified by their Westerlund (1987) designation.

2007). This could have different reasons: The most obvious one would be simply statistics. Using only four stars before, statistic uncertainties are severe. The new value should be somewhat more reliable in that respect, but here the nature of the additional stars could introduce additional velocity dispersion. According to de Jager (1998), YHGs undergo radial pulsations, which can cause variations in radial velocity of up to  $\approx \pm 7\text{km/s}$ . Literature on spectral variations of YHGs is scarce, but from what is known, it seems easily possible that an increase in velocity dispersion of a few km/s could originate from this.

The other parameter we require for the determination of the dynamical mass is the projected half-light radius. We used the NIR image we created from the archival NTT/SOFI data to obtain a radius which contains half of the total light (in projection) to be  $r_{hp} = 0''.86 \pm 0''.14$ . The uncertainty comes mostly through assumption of different locations of the weakly constrained cluster centre. This value is consistent with the half-mass radius of 1pc (for stellar masses between  $3.4$  and  $32 M_{\odot}$ ) presented by Brandner et al. (2007).

The resulting dynamical mass, for a cluster in Virial equilibrium, is (assuming  $\eta = 9.3$ , for details on the formula see Mengel et al. (2002))

$$M_{dyn} = \eta \sigma^2 r_{hp} / G = 1.5_{-0.7}^{+0.9} \times 10^5 M_{\odot}$$

Within the uncertainties, this is consistent with that found by Clark et al. (2005), and somewhat higher than the mass determined by Brandner et al. (2007). Both use stellar counts of the current population (with detection of the main sequence only in the latter publication) to infer an initial cluster mass using an assumed stellar initial mass function.

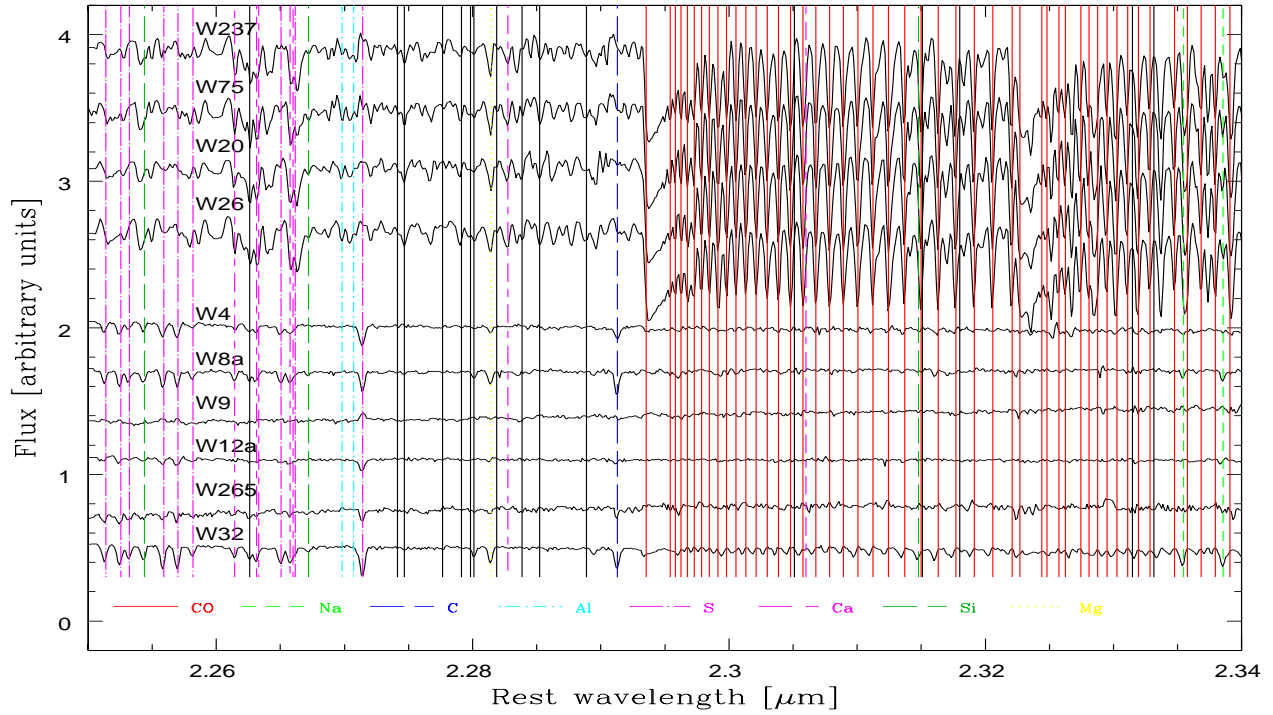


**Fig. 2** Spectra of integrated cluster and the near-infrared brightest individual stars. Atmospheric absorption (corrected for, but over-compensation and sub-optimal sky subtraction causes a few artefacts at long wavelengths) is shown at the bottom. Line identifications taken from Hinkle et al. (1995).

In Mengel & Tacconi-Garman (2007), we used the relative numbers of the stellar populations, together with evolutionary synthesis models, (Leitherer et al. 1999; Vazquez & Leitherer 2005) to age date the cluster. We determine the best fitting age to be 5 Myrs.

We used different methods (with reasonable agreement) to determine  $L_V$  for the cluster: Using the integrated, extinction corrected K-band magnitude and the Starburst99 V-K colour at 5 Myr, or the integrated V-band magnitude with (substantial) extinction correction, or the luminosity expected from Starburst99 for the cluster mass of  $10^5 M_\odot$  expected from stellar counts. A total luminosity of  $L_V \approx 5.8 \times 10^6 L_\odot$  leads to a light-to-mass-ratio of  $L_V/M_{dyn} \approx 40$ .

Having added our data point in the diagnostic Figure 3, taken from Goodwin & Bastian (2006), we find that Wd 1 is located between the model lines denoting a star formation efficiency of 40% and 50%. Both of these efficiencies, in the N-body models of Goodwin & Bastian (2006), lead to the formation of stellar clusters which eventually, after 10-15 Myr, re-establish virial equilibrium. This means that, based our data, Wd 1 does not seem to be currently in the process of dissolution. The potential influence of radial pulsations in the YHG suggests that the velocity dispersion and hence the virial cluster mass may be overestimated. On the other hand,

mass segregation could have biased our measurements, both the velocity dispersion, and the cluster size, towards values which are too low.

#### 4 Conclusions and future work

1. We identify ten stars which allow a determination of radial velocity in the part of the K-band which we use for our spectral analysis: four RSGs, five YHGs, and one emission line star. The rms velocity dispersion of these stars was found to be  $9.2 \pm 2.5$  km/s. The resulting dynamical mass is  $1.5^{+0.9}_{-0.7} \times 10^5 M_\odot$ .
2. There is no indication of cluster dissolution. Comparing  $L/M$  to theoretical expectations suggests a star formation efficiency between 40 and 50%, which is compatible with the cluster re-establishing equilibrium after the phase of gas expulsion.
3. We cannot rule out systematic or statistical errors in our analysis yet, since the sample of stars, even though larger than before, with just ten stars is still quite small. Furthermore, our measurements may have suffered a bias from either pulsations of the YHGs (velocity dispersion, and hence mass, would be too high), or by not taking into account potential

mass segregation (velocity dispersion and size, and hence mass, would be too low).

It is rather straightforward to overcome the potential problems mentioned: For better statistics, we need to have access to more radial velocity determinations. We were granted observing time to observe other stellar types in a different near infrared wavelength region. Furthermore, we will observe two additional epochs, which will give us an indication of the impact of radial pulsation in the YHG. And finally, there are two ways to address mass segregation: Brandner et al. (2007) see some indication of mass segregation in their SOFI data. Once deeper NIR imaging data, which already exist, are analyzed, an even better estimate of this property will be possible. Our new spectra will also cover lower mass stars, which will allow us to check if their velocity dispersion is lower than that of the lower mass stars.

All of these future investigation will help settle the question conclusively if Westerlund 1 will dissolve within the next 10-20 Myr or not - an important step towards understanding what fraction of the galactic stellar population originates in star clusters.

## 5 Questions and answers

Mark Gieles: Perhaps there is some evidence for mass segregation: If the high mass stars sink to the centre, they will speed up, because they move deeper in the potential. Of course, this argument works only if you can confirm that your massive stars are also more centrally concentrated.

Sabine Mengel: At the time of the presentation, deep NIR imaging data had not been published yet, and therefore the main sequence had been undetected and no information regarding mass segregation was available. In the meantime, Brandner et al. (2007) published their SOFI images, and they believe that they see some indication for mass segregation, however it is not quite clear for me yet if this conclusion is unaffected by statistical and/or observational bias. It is however believed that the high mass stars segregate because they lose energy, and that they move more slowly than the low mass stars, once they are segregated.

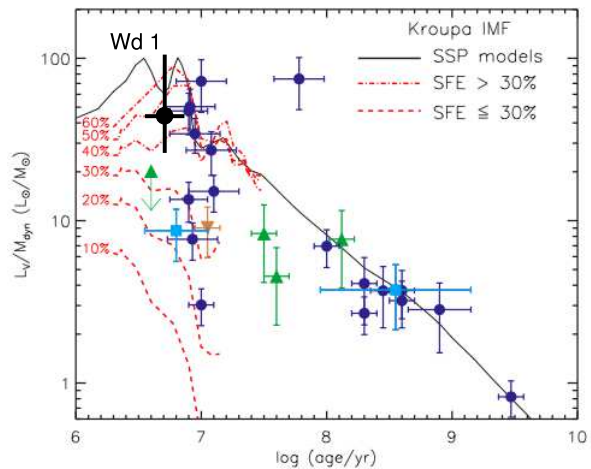


**Fig. 3** Evolution of  $L/M_{dyn}$  for clusters with variable star formation efficiencies (modified version of a diagram taken from Goodwin & Bastian (2006)). Clusters with an effective star formation efficiency of below  $\approx 40\%$  dissolve after around 10 Myr. Wd1 (the black cross) is located in a region which would correspond to a star formation efficiency of around 45%, and hence appears stable against (rapid) dissolution.

---

## References

- Bastian N., Gieles M., Lamers H.J.G.L.M., Scheepmaker R.A., de Grijs R., 2005, *A&A*, 431, 905
- Brandner W., Clark J.S., Stolte A., Waters R., Negueruela I., and Goodwin S.P., 2007, astro-ph 0711.1624
- Clark J.S., Negueruela I., Crowther P.A., and Goodwin S.P., 2005, *A&A*, 434, 949
- Crowther P.A., Hadfield L.J., Clark J.S., Negueruela I., Vacca W.D., 2006, *MNRAS*, 372, 1407
- de Jager C., 1998, *A&AR*, 145
- Fall S.M., 2004, ASP Conference Series, Vol. 322. Edited by H.J.G.L.M. Lamers, L.J. Smith, and A. Nota. San Francisco: Astronomical Society of the Pacific, 2004., p.399
- Goodwin S.P. & Bastian N., 2006, *MNRAS*, 373, 752
- Hinkle K., Wallace L, & Livingston W., 1995, *PASP*, 107, 1042
- Holtzman J. A. et al. 1992, *AJ*, 103, 691
- Leitherer, C., et al. 1999, *ApJS*, 123, 3
- Mengel S., Lehnert M.D., Thatte N., & Genzel R., 2002, *A&A*, 383, 137
- Mengel S., Lehnert M.D., Thatte N., & Genzel R., 2005, *A&A*, 443, 41
- Mengel S. & Tacconi-Garman L.E., 2007, *A&A*, 466, 151
- Rousselot P., Lidman C., Cuby J.-G., Moreels G., & Monnet G., 2000, *A&A*, 354, 1134
- Vazquez G.A. & Leitherer C., 2005, *ApJ*, 621, 695
- Westerlund B.E., 1961, *PASP*, 73, 51
- Westerlund B.E., 1987, *A&AS*, 70, 311
- Whitmore B.C., and Schweizer F, 1995, *AJ*, 109, 960
- Whitmore B.C., Chandar R., and Fall S.M., 2007, *AJ*, 133, 1067